Carbohydrate Polymers 105 (2014) 63–69

Contents lists available at ScienceDirect

Carbohydrate Polymers

journal homepage: www.elsevier.com/locate/carbpol

In situ cross-linked polysaccharide hydrogel as extracellular matrix mimics for antibiotics delivery

Yu Zhao [a], Xinge Zhang [a,*], Yanan Wang [a], Zhongming Wu [b], Jinxia An [a], Zhentan Lu [a], Lin Mei [a], Chaoxing Li [a]

[a] Key Laboratory of Functional Polymer Materials of Ministry Education, Institute of Polymer Chemistry, Nankai University, Tianjin 300071, China
[b] Metabolic Disease Hospital, Tianjin Medical University, Tianjin 300070, China

ARTICLE INFO

Article history:
Received 16 October 2013
Received in revised form
17 December 2013
Accepted 20 January 2014
Available online 29 January 2014

Keywords:
Hydrogel
Polysaccharide
Antibacterial
Wound dressing

ABSTRACT

Many synthetic hydrogels for drug delivery have been based on polyethylene glycol which is non-natural, non-biodegradable and only terminal-functionalizable. The polysaccharides dextran and chitosan not only are highly hydrophilic, biodegradable and pendant-functionalizable, but also more closely mimic the nature extracellular matrix glycosaminoglycans. Here, a biomimetic hydrogel based on chitosan and dextran was synthesized by the Michael addition reaction. The hydrogels have good swelling and cytocompatibility against NIH3T3. Moreover, vancomycin-loaded hydrogels were formed in situ, and could kill both Gram-positive bacteria and Gram-negative bacteria, indicating that the hydrogel as a wound dressing could provide protection against bacterial infection. Notably, the drug release was controlled via modifying the compositions. Therefore, the biomimetic polysaccharide hydrogels as a promising carrier have potential application for wound healing.

1. Introduction

The skin plays an important role in human body and prevents from being infected by microbes. Skin generally needs to be covered with a dressing immediately after it is damaged (Jayakumar, Prabaharan, Kumar, Nair, & Tamura, 2011). Wound healing typically occurs through the process of hemostasis, inflammation, tissue repair and remodeling. Conventional wound dressings such as bandages, gauze and foam dressing just cover the surface of the wound and absorb tissue exudates. However they cannot provide an appropriate environment for tissue repair and regeneration, easily adhere to wound and damage the new epithelial tissue leading to bleeding. Advanced dressings, including biological and synthetic scaffolds, can provide a physical barrier against secondary infection, as well as a compatible physiological environment (Song, Rane, & Christman, 2012). Wound infection is the major difficulty in the field of wound care management, because such infection can cause to form exudate, delay the wound healing, facilitate improper collagen deposition, etc. (Kumar et al., 2012; Madhumathi et al., 2010; Paul & Sharma, 2004). Hydrogels are soft and wet materials that contain a large amount of water for their three dimensional polymer network structure. Besides the applications such as drug delivery system, contact lenses, corneal implants, and as scaffolds for tissue engineering (Haque, Kurokawa, & Gong, 2012), they have been utilized as promising materials for wound healing, surgical tissue adhesives, and hemostasis during surgery as well as for local drug delivery depots (Ryu et al., 2011; Zhang, Qadeer, & Chen, 2011). Moreover, interpenetrated polymer networks have shown the promise as a way of incorporating antimicrobial agent into polymer such as the antibiotic streptomycin sulfate (Song et al., 2012) or tetracycline (Paul & Sharma, 2004) where the polymer networks act as a carrier for the antibiotics delivery system.

Chitosan is a modified natural polysaccharide derived from chitin and one of the rare natural-based cationic polymers (Schutz, Juillerat-Jeanneret, Kauper, & Wandrey, 2011). It has been widely used in biomedical field due to their bioactivity, biodegradability, biocompatibility, low toxicity and bacteriostatic effect (Bhattarai, Gunn, & Zhang, 2010; Brunel et al., 2009, 2010; Mao, Sun, & Kissel, 2010; Wu, Shen, Banerjee, & Zhou, 2010). The antibacterial activity of its derivatives against *E. coli* and *S. aureus* was affected by the degree of *N*-substitution and molecular weight, especially in the range between 5 and 10 kDa (Sajomsang, Gonil, & Tantayanon, 2009; Sajomsang, Tantayanon, Tangpasuthadol, & Daly, 2009; Tsao et al., 2010). Dextran is highly hydrophilic and has high molecular weight resulting in relatively good mechanical property (Rokhade, Patil, & Aminabhavi, 2007). Moreover, dextran is a natural biodegradable polysaccharide with abundant pendant hydroxyl groups amenable to chemical modification. More

* Corresponding author. Tel.: +86 22 23501645; fax: +86 22 23505598.
E-mail address: zhangxinge@nankai.edu.cn (X. Zhang).

0144-8617/$ – see front matter © 2014 Elsevier Ltd. All rights reserved.
http://dx.doi.org/10.1016/j.carbpol.2014.01.068

importantly, the polysaccharide dextran is chemically similar to glycosaminoglycan which is an important constituent of extracellular matrix (ECM). We postulate that combination of chitosan and dextran in a composite hydrogel could more closely mimic the natural structure and function of ECM. In our previous study (Teng et al., 2010), the hydrogel based on thiolated chitosan and polyethylene glycol (PEG) was synthesized by the Michael type addition reaction, and the hydrogels have been used for drug delivery and cell tissue engineering.

Here, the hydrogels based on thiolated chitosan and maleic acid-grafted dextran were developed. The cell viability, swelling, drug encapsulation and release behaviors were tracked. Finally, the antibacterial property of drug-loaded hydrogels was further explored. We expect that the polysaccharide hydrogel as a wound dressing could promote wound healing.

2. Materials and methods

2.1. Materials

Chitosan (CS) was purchased from Golden-Shell Pharmaceutical Co. Ltd., Jiangsu, China. Dextran (Dex) was purchased from Sinopharm Chemical Reagent Co. Ltd., Beijing, China and dried under vacuum at 60 °C before used. 1-Hydroxybenzotriazole (HOBt) and 1-(3-dimethylaminopropyl)-3-ethylcarbodiimide hydrochloride (EDAC·HCl) were purchased from Medpep Co. Ltd., Shanghai, China. *N*-Acetyl-L-cysteine (NAc) was purchased from Alfa Aesar, USA. Maleic anhydride (Ma), triethylamine (TEA) and isopropyl alcohol (IPA) were purchased from Chemical Reagent Co. Ltd., Tianjin, China. 5,5′-Dithiobis (2-nitrobenzoic acid) (DTNB) and 3-(4,5-dimethylthiazol-2-yl)-2,5-diphenyltetrazolium bromide (MTT) were purchased from Sigma–Aldrich, USA. Dulbecco's modified eagle's medium (DMEM), heat-inactivated fetal bovine serum (FBS) and trypsin were purchased from Gibco, USA. Vancomycin was purchased from Aladdin, Shanghai, China.

2.2. Preparation of thiolated chitosan (CS-NAc)

N-Acetyl-L-cysteine conjugated chitosan (CS-NAc) was obtained according to the method reported by our group (Wang et al., 2009). Briefly, 500 mg of CS and 377 mg of HOBt were dispersed in water under stirring. Then 4286 mg of EDAC·HCl and 912 mg of NAc were added to the above solution. PH of the reaction mixture was adjusted to 5 using 1 M HCl, then reacting in the dark for 3 h. The resultant mixture was dialyzed (10 kDa cutoff) first against 5 mM HCl containing 2 μmol/L EDTA at 4 °C for 72 h in the dark, then 5 mM HCl containing 1% of NaCl, finally 1 mmol/L HCl before the solution was freeze dried. Thiol content was determined using Ellman's reagent as described by Krauland, Leitner, and Urch (2003). The main chemical shift of CS-NAc: Fig. S1 showed the ^{1}H NMR (400 MHz, D_2O, TMS): 4.94 (s, H-6), 3.99 (s, H-1, H-2), 3.83 (s, H-3, H-4), 3.24 (s, H-5), 2.97 (s, —S—CH_2—), 2.07 (s, —$COCH_3$). According to Fourier transform infrared (FTIR) result of CS-NAc, when compared with chitosan, a stronger absorption peak at 1654 cm^{-1} (amide I band) which was assigned to carbonyl in amide, indicating that NAc was introduced into chitosan successfully.

2.3. Preparation of maleic acid-grafted dextran (Dex-Ma)

Maleic acid-grafted dextran (Dex-Ma) was synthesized according to the method described by Kim, Won, and Chu (1999). Briefly, dextran was dissolved in 20 mL of DMF containing 2 g of LiCl at 90 °C under nitrogen. TEA was added to the solution as a catalyst at 60 °C and maleic anhydride was subsequently added. The reaction mixture was generally conducted at 60 °C for 10 h. The reaction mixture was precipitated in 50 mL of cold isopropyl alcohol, washed three times with isopropyl alcohol, and dried at room temperature under vacuum for a week and stored in cold dark before used. The degree of substitution of Dex-Ma was 55%, determined by acid-base titration. FTIR result of Dex-Ma shows that the peak at 1722 cm^{-1} was ascribed to carboxyl, and the peak at 1661 cm^{-1} was assigned to carbon–carbon double bound comparing with dextran. The ^{1}H NMR peaks at 6.3 and 6.6 ppm were protons of the double bond of maleic acid.

2.4. Preparation and characteristics of CNDM hydrogel

To determine the gelation time, the solution of CS-NAc and Dex-Ma (the molar ratio of thiol group to maleic group, 1:3, 1:2, 1:1, 2:1 and 3:1) in phosphate buffer solution (PBS, pH 7.4, 0.02 M) were incubated at 37 °C by vortexing. The gelation time was determined by a flow test utilizing a glass test tube inverting method reported by Jeong, Bae, and Kim (1999). As the solution lost fluidity in 1 min, the sample was regarded as a gel.

FTIR spectroscopy of the sample was performed with FTS 6000 spectrometer (Bio-Rad, USA). The dried samples were mixed with KBr and tableted. To examine thermal stability of hydrogels, the samples were measured using thermogravimetric analysis (TGA, Metzsh). Decomposition profiles of TGA were recorded with a heating rate of 10 °C/min in nitrogen between 20 and 450 °C.

2.5. Morphology of hydrogels

To observe the morphology of hydrogels, the synthetic hydrogels were quickly frozen in liquid nitrogen and further freeze-dried in a Freeze Drier (FTS SYSTEMS, USA) in vacuum at −90 °C for 36 h until all the solvent was sublimed. The freeze-dried hydrogels were then fractured carefully, and the interior morphology of the hydrogels were visualized by using a scanning electron microscope (SEM, Shimadzu SS-550, Japan) (Teng et al., 2010). Before the SEM observation, the hydrogel samples were fixed on conductive tape and coated with gold.

2.6. Swelling ratio of hydrogels

To understand the effect of the molecular transport of liquids into hydrogels on the drug release, swelling measurement was carried out by immersing the hydrogels in PBS (pH 7.4) at 37 °C. At predetermined time intervals, the samples were taken out and wiped carefully between tissue papers to remove the surface-adhered liquid droplets, and then weighted on an electron microbalance (AE 240, Mettler, Switzerland) to an accuracy of ±0.1 mg. Each sample was performed in triplicate, and average value was calculated for data analysis. The percentage of equilibrium water uptake was calculated as follows:

$$\text{Swelling ratio} = \frac{W_t - W_0}{W_0}$$

where W_t is the weight of swollen hydrogels, and W_0 is the initial weight of hydrogels.

2.7. The cell viability

Mouse fibroblast NIH3T3 cells were maintained in DMEM medium supplemented with 10% heat-inactivated fetal bovine serum (FBS), 100 mg/L streptomycin, and 100 IU/mL penicillin. Cells were grown in a 25 mL cell culture flask and incubated at 37 °C in a humidified atmosphere of 5% CO_2 to approximately 70–80% confluence. After a subculture was performed every 2–3 days, medium

was removed to eliminate the dead cells, and the adherent cells were detached from the surface of the culture flask by trypsinization.

Cytotoxicity of the hydrogels was assessed by the MTT method (Dutta, Shome, Kar, & Das, 2011; Mitra, Shome, Paul, & Das, 2009; Roy & Das, 2008). First, 8 mg hydrogels was incubated in 8 mL of pH 7.4 PBS for 72 h, and then filtrated. Second, NIH3T3 cells in the logarithmic growth phase (the number of viable cells > 99%) were digested with 0.25% trypsin. A concentration of 5×10^4 cells per milliliter of cell suspension was prepared. 100 μL of cell suspension was added rapidly to a 96-well plate. Then, the 96-well plates were put in 5% CO_2/95% O_2 incubator to cultivate 24 h. After 24 h of incubation, the medium was replaced with the different concentrations of leaching solution (4, 2, 1 and 0.5 mg/mL), the control group only added an equal amount DMEM medium cultured in 5% CO_2/95% O_2 incubator for 24 and 48 h, respectively. Then, 10 μL of MTT solution (5%) in PBS was added to the above mixture, and the cells were further incubated for another 4 h. The precipitated formazan was dissolved thoroughly in DMSO, and absorbance at 545 nm was measured using Microplate Reader (Molecular Devices, USA). The number of surviving cells was expressed as percent viability = $(A_t - A_0)/(A_c - A_0) \times 100\%$. Where A_t is the absorbance of treated cell, A_c is the absorbance of controlled cell and A_0 is the absorbance of PBS.

2.8. Fabrication of vancomycin-loaded hydrogels

Being different from the previous method to construct drug-loaded hydrogel, we tried a new plan to encapsulate vancomycin into hydrogels. First, 9 mg vancomycin was added to 10 mL of PBS, then CS-NAc and Dex-Ma were dissolved in the solution and the mixture was incubated at 37 °C by vortexing to obtain drug-loaded hydrogels. In this case, the drug loading ability was considered to be 100%.

2.9. In vitro drug release

Typically, vancomycin-loaded hydrogels (10 mg) was placed in 2 mL of pH 7.4 PBS with shaking at 37 °C. At appropriate time-points, the aliquots of 100 μL supernatant were withdrawn and replaced by fresh buffer solution. The amount of vancomycin was measured using an UV spectrophotometer (Shimadzu UV2550, Japan) at a wavelength of 280 nm (Zhang et al., 2008).

2.10. Antibacterial assay

LIVE/DEAD assay was used to evaluate the antibacterial property of the hydrogels. 10^6 Colony Forming Units (CFU) mL^{-1} of both *S. aureus* and *E. coli* were co-cultured with hydrogels for 1 h, respectively. A solution of LIVE/DEAD staining fluorescence dye, acridine orange (0.1 mg) and ethidium bromide (0.1 mg), in 100 μL of pH 7.4 PBS was added to the hydrogels. After 15 min, the hydrogels were washed three times with PBS, and then 40% glycerol solution was used to suspend the stained bacteria. The live/dead bacteria were observed under a fluorescence microscope (Leica DMI4000B, Germany).

The morphological changes of bacteria were observed by field emission scanning electron microscope (FESEM) before and after the treatment of hydrogels (Chen et al., 2010). *E. coli* and *S. aureus* were cultured to an exponential phase and then harvested by centrifugation, followed by washing twice with PBS and resuspended in it. Bacteria were incubated at 37 °C for up to 60 min with 10 mg hydrogels (unloading and loading vancomycin). Controls were performed in the absence of hydrogels. Cells were fixed with 2.5% (w/v) glutaraldehyde in PBS, washed extensively with PBS, and then dehydrated with a graded ethanol series (30%, 50%, 70%, 95% and 100%, 15 min each). After freeze-drying and gold coating, the samples were observed with FESEM (JEOL-JSM7500, Japan).

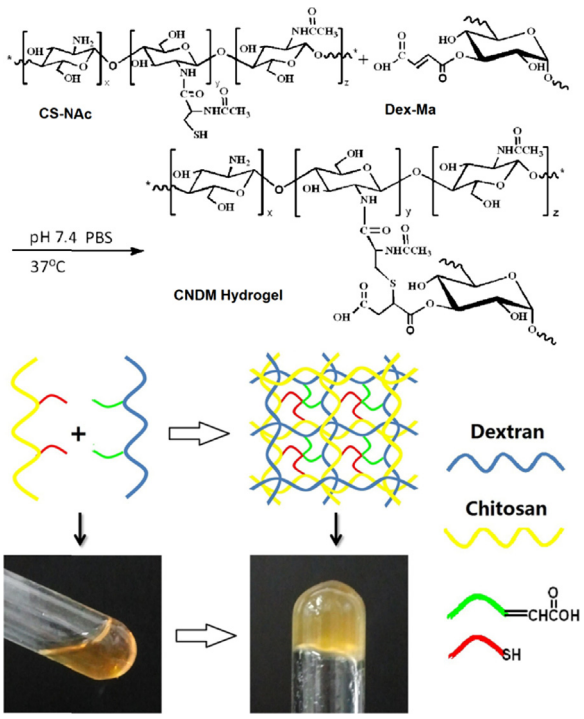

Scheme 1. Scheme of CNDM hydrogel formation.

3. Results and discussion

3.1. In situ formation and characterization of hydrogels

CS-NAc was obtained by the covalent attachment of NAc to the amine groups of CS. The coupling reaction was mediated by EDAC and HOBt according to our method previously reported (Wang et al., 2009). In the present work, we used the most appropriate NAc/EDAC molar ratio, and the content of free thiol group was about 200 μmol/g determined by Ellman's assay.

To obtain the in situ forming hydrogels, CNDM hydrogel was prepared by the incubation of CS-NAc and Dex-Ma in pH 7.4 PBS at 37 °C (Scheme 1). Moreover, Michael type addition between thiol group and maleic group easily happened. To determine the gelation time, the hydrogels with different concentrations and compositions were synthesized. As shown in Table 1, at the same molar ratio of thiol to maleic group, the gelation time of CN1DM1 decreased from 12 to 0.2 h as the content of CS-NAc and Dex-Ma increased from 40 to 150 mg/mL. However, we found that the gelation time

Table 1
Gelation time of the hydrogels with different compositions and concentrations.

Hydrogel	Molar ratio of thiol to maleic acid	Mass percentage of Dex-Ma (%)	Material concentration (mg/mL)	Gelation time (h)
		15.5	40	12
		15.5	50	6
CN1DM1	1:1	15.5	75	3
		15.5	100	1.1
		15.5	150	0.2
CN1DM2	1:2	27.0	100	1.4
CN1DM3	1:3	36.0	100	1.2
CN1DM3	1:3	36.0	150	0.3
CN2DM1	2:1	8.5	100	1.2
CN3DM1	3:1	6.0	100	1.4

was the shortest when the molar ratio of thiol to maleic is 1:1 at the same content of materials. At the same content of material (100 mg/mL), the gelation time was hardly affected by the molar ratio of thiol to maleic. FTIR result in Fig. S2 shows that the peak at 1661 cm^{-1} ascribed to carbon–carbon double bond in CNDM hydrogels disappeared, suggesting that thiol group of CS-NAc reacted with double bond of Dex-Ma through Michael type addition.

3.2. Thermal stability of CNDM hydrogel

Thermal stabilities of CNDM hydrogels were evaluated, TG and DTG curves for CS-NAc, Dex-Ma and CNDM are shown in Figure S3. For CS-NAc, there were two stage weight loss in the range of 40 and 300 °C. The first one with a weight loss of 6% was assigned to free water and water linked through hydrogen bonds, which were released in the 30–40 °C region and reached a maximum at 40 °C; the second point of a weight loss of 28%, up to 236 °C, corresponded to the decomposition (thermal and oxidative) of CS and vaporization and elimination of volatile products. Dex-Ma also showed two stage weight loss in the range of 110 and 250 °C. The weight loss of 7% at 110 °C was assigned to the release of free water and water linked through hydrogen bonds; the second weight loss of 42% was the breaking of dextran chains. It is known that pyrolysis of polysaccharides starts by a random split of the glycosidic bonds, followed by further decomposition forming acetic bonds, followed by further decomposition forming acetic and butyric acids and a series of lower fatty acids, where C2, C3, and C6 predominate (Neto et al., 2005). Moreover, variations on the peak area and position related to water loss were expected to reflect physical and molecular changes caused by the modification of cross-linking with dextran. For CNDM hydrogels, there were differences in peak area and position, indicating that hydrogel differed in the water holding capacity and in the strength of water–polymer interaction. Such changes might clearly indicate the distinct formation of hydrogels. Fig. S3a showed the weight loss with maxima at 23% for CNDM hydrogels, indicating an increase in sample thermal stability compared with chitosan and dextran, this behavior was probably due to the formation of the carbon–sulfur bonds.

3.3. Morphology of hydrogels

The morphologies of the swollen CNDM hydrogels in PBS at 37 °C were observed by SEM. As shown in Fig. 1A and B, the SEM images of hydrogels exhibited a highly macroporous spongelike structure and the average mesh size was about 15 μm. With the increase of cross-linking density, the decrease of the pore size was attributed to the reducing distance between CS and Dex. After being dipped in PBS for a week, the chains in the network degraded and pore size of the hydrogel increased (the data were not shown). Importantly, the hydrogels with porous structure had interior space to receive the microbe and then react with drug loaded in the hydrogel pores (Li et al., 2011).

3.4. Swelling assay

Hydrophilicity is an important characteristic of the hydrogels. Excellent water uptake ability of a material facilitates both cell attachment and penetration during in vitro cell culturing. To determine their hydrophilicity, we explored the swelling of CNDM hydrogels. Fig. 2 showed swelling kinetic curves of the hydrogel in pH 7.4 PBS at 37 °C. All these hydrogels almost reached full swelling ratio after 1 h incubation, and the average swelling ratio was about 250%. For the hydrogels with 100 mg/mL of material concentration, the swelling ratio increased from 200% to 270% when the

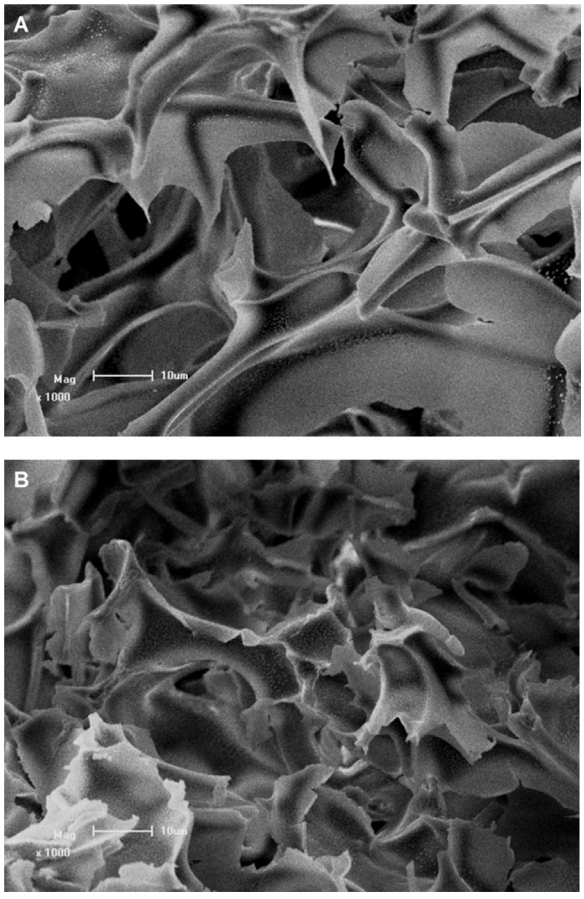

Fig. 1. SEM images of CNDM hydrogel: (a) CN1DM3 hydrogel, and (b) CN1DM3 (150) hydrogel.

mole ratio of thiol group to maleic group increased from 1:1 to 1:3, indicating that Dex-Ma played an important role in the water uptake of CNDM hydrogels. For CN1DM3 hydrogels, the equilibrium swelling ratio increased from 300% to 340% when enhanced the concentration from 100 to 150 mg/mL. We generally believed that the hydrogels prepared at a high concentration had a tighter structure and a higher water-holding capacity. This also indicates that dextran has an important influence on the hydrogels swelling. However, at the same the material content, the hydrogels whose ratios of thiol group and maleic group of 1:1, 2:1 and 3:1 had the

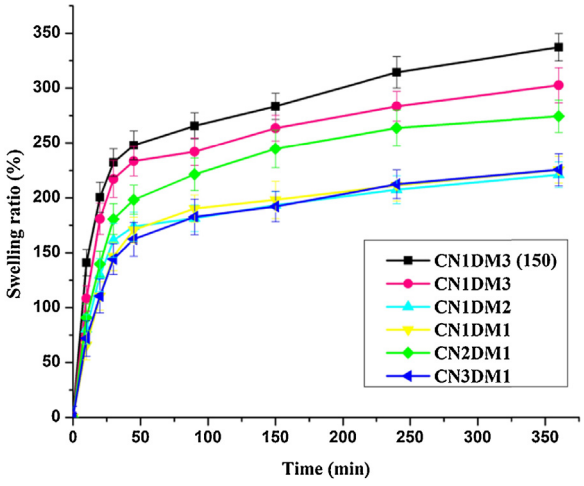

Fig. 2. Swelling kinetic curves of hydrogels at 37 °C in PBS pH 7.4 (mean ± S.D., $n = 3$).

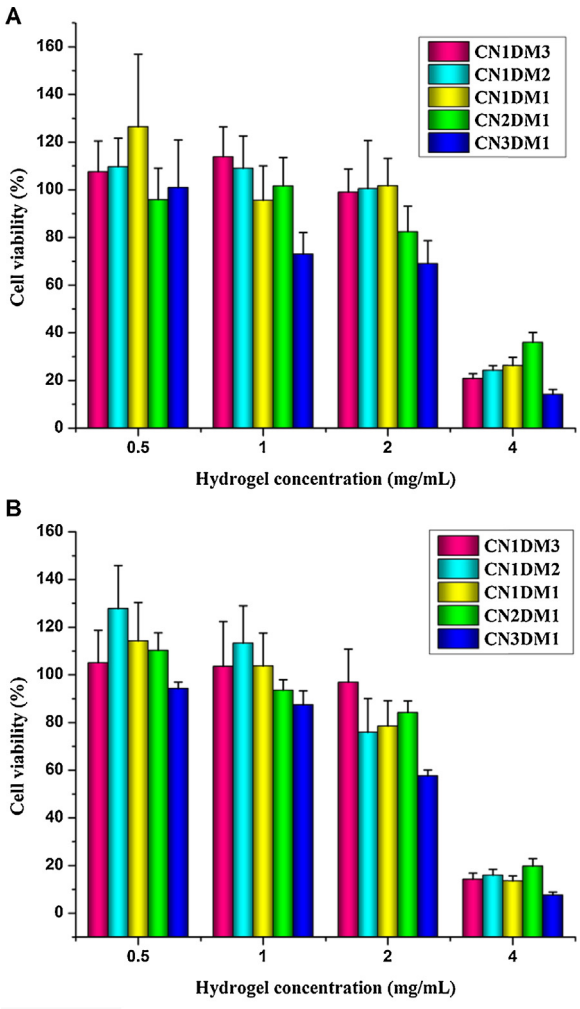

Fig. 3. Cell viability after incubation as a function of CNDM hydrogel concentrations determined by MTT assay for 24 (A) and 48 h (B). Each value represents the mean ± SD ($n = 5$).

same swelling ratio, suggesting that dextran played important role in the swelling of CNDM hydrogels again, which maybe because CS with the high molecular weight was difficult to dissolve in pH 7.4 PBS.

3.5. Cell viability

The potential for CNDM hydrogels as antibacterial wound dressing was further assessed with the MTT assay. The cytocompatibility of CNDM hydrogels was evaluated in vitro on NIH3T3 cells by "indirect" method. In this method, the growth medium was first "conditioned" for 5 days with the hydrogels and then used to incubate the cells. After 24 and 48 h of incubation, cell viability was determined by the MTT assay and expressed as a percentage ratio between viable cell number incubated in the growth medium "conditioned" and not "conditioned" by the hydrogel.

The result of MTT assay shows that the cytotoxicity of the hydrogels against NIH3T3 increased with hydrogels concentration rising (above 2 mg/mL, Fig. 3A and B). However, the cell viability was more than 80% at lower than 2 mg/mL, suggesting that the cell proliferated even in the presence of hydrogels. Notably, the cell viability increased with culture time, indicating that some substances promoted the cell growth (Fig. 3B). The cytotoxicity, however, increased by chitosan with positive charge at high concentration. These results indicate that the hydrogels had low cytotoxicity and

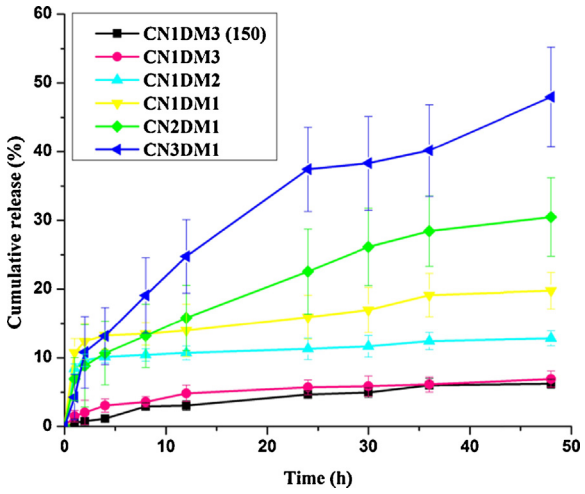

Fig. 4. In vitro percentage cumulative release of vancomycin from CNDM hydrogels at 37 °C in pH 7.4 PBS. Each hydrogel was analyzed and each datum point represents the mean value ± S.D. ($n = 3$).

contributed to cell proliferation, which could promote wound healing.

3.6. Drug release

Vancomycin release in vitro was determined using an UV spectrophotometer. As shown in Fig. 4, vancomycin released from the hydrogels in a sustained manner. Moreover, the release behavior of drug-loaded hydrogels showed a similar trend. However, the amount of released drug increased as dextran content in hydrogels decreased, indicating drug release behavior depended on the drug-hydrogel interaction. For CN1DM1 and CN1DM2 having the obvious burst release, the release amount was up to 20% and 12% during the initial 48 h, respectively. However, for CN2DM1 and CN3DM1 hydrogels, the release amount was up to 30% and 48% at the same time, respectively. The drug release amount from hydrogels CN1DM3, however, was only 6% during the initial 48 h. Combination of the hydrogel composition (weight percentage of Dex-Ma to CNDM hydrogel) in Table 1, we found that the effect of dextran on drug release was significant. This maybe because hydroxyl groups of vancomycin could strongly interact with Dex-Ma through hydrogen bond, so the more Dex-Ma in hydrogel, the lower amount of vancomycin released.

Inspired by the works of Aminabhavi's group (Agnihotri & Aminabhavi, 2007; Mundargi, Patil, & Aminabhavi, 2007; Mundargi, Shelke, Rokhade, Patil, & Aminabhavi, 2008; Rokhade, Patil, et al., 2007; Rokhade, Shelke, Patil, & Aminabhavi, 2007), we further analyzed the in vitro release mechanism of vancomycin. To determine the mechanism, the following Ritger–Peppas ($M_t/M_\infty \leq 60\%$) equation was used to fit the data of cumulative release (Zalfen et al., 2008).

$$\frac{M_t}{M_\infty} = Kt^n$$

where M_t/M_∞ is the fraction of drug released at time t, K is a kinetic rate constant characteristic of the polymer–drug interaction and n is the diffusional exponent characterizing the release mechanism. If $n < 0.46$, Fickian diffusion occurs; if $0.46 < n < 0.89$, it suggests anomalous (non-Fickian) transport and for $n = 0.89$ zero-order release is possible and if $n > 0.89$, super-Case-II transport is operative (Mundargi et al., 2007, 2008).

The fitting data are shown in Table 2, the n values of CN1DM3, CN1DM2, CN1DM1, CN2DM1 for the release of vancomycin were

Table 2
Drug release kinetic data for CNDM hydrogel obtained from fitting drug release experimental data to Ritger–Peppas equation (n: diffusion exponent; K: kinetic constant; R^2: correlation coefficient).

Sample	$M_t/M_\infty = Kt^n$			Transport mechanism
	K	n	R^2	
CN1DM3 (150)	0.54	0.67	0.97	Non-Fickian diffusion
CN1DM3	1.62	0.39	0.98	Fickian diffusion
CN1DM2	8.67	0.09	0.95	Fickian diffusion
CN1DM1	10.65	0.14	0.91	Fickian diffusion
CN2DM1	6.46	0.40	0.98	Fickian diffusion
CN3DM1	5.65	0.57	0.96	Non-Fickian diffusion

lower than 0.46, indicating that release mechanism of drug was mainly Fickian diffusion. However, for CN1DM3 (150) and CN3DM1, the n value was higher than 0.46, suggesting that release mechanism of drug from CN1DM3 (150) and CN3DM1 was Fickian diffusion and polymer chain relaxation. The difference of drug release mechanism between CNDM hydrogels was probably influenced by the degree of cross-linking (Agnihotri & Aminabhavi, 2007; Rokhade, Patil, et al., 2007; Rokhade, Shelke, et al., 2007) and hydrogen bond between Dex and vancomycin.

3.7. Antibacterial activity

The LIVE/DEAD bacterial viability assay was further performed with *E. coli* and *S. aureus* stained by AO&EB fluorescent dyes. In this assay, bacterial cells that looked green/red were live/dead with intact/damaged membranes when visualized by fluorescence microscopy. Fig. 5A showed fluorescence micrographs of *E. coli* and *S. aureus* treated with blank and drug-loaded CNDM hydrogels. For the control group, bacterial cells fluoresced green (Fig. 5Aa and 5Ad), indicating that these cells were alive. After treated with the drug-loaded hydrogels for 60 min, all bacterial cells presented red. However, the blank hydrogels, some of *E. coli* presented red while *S. aureus* still presented green, indicating that the hydrogel has a antibacterial activity against Gram-negative bacteria, because Gram-negative bacteria contained an outer membrane wherein lipopolysaccharide and proteins were held together by electrostatic interactions with bivalent metal ions, 1–2 layers of peptidoglycans (cell wall), and a cell membrane (containing lipid bilayer, trans-membrane proteins, and inner/outer membrane proteins); the negatively charged O-specific antigenic oligosaccharide repeating units of the *E. coli* lipopolysaccharide form an ionic-type of binding with the positive charged amino groups of chitosan, thus blocking the nutrient flow with bacterial death due to depletion

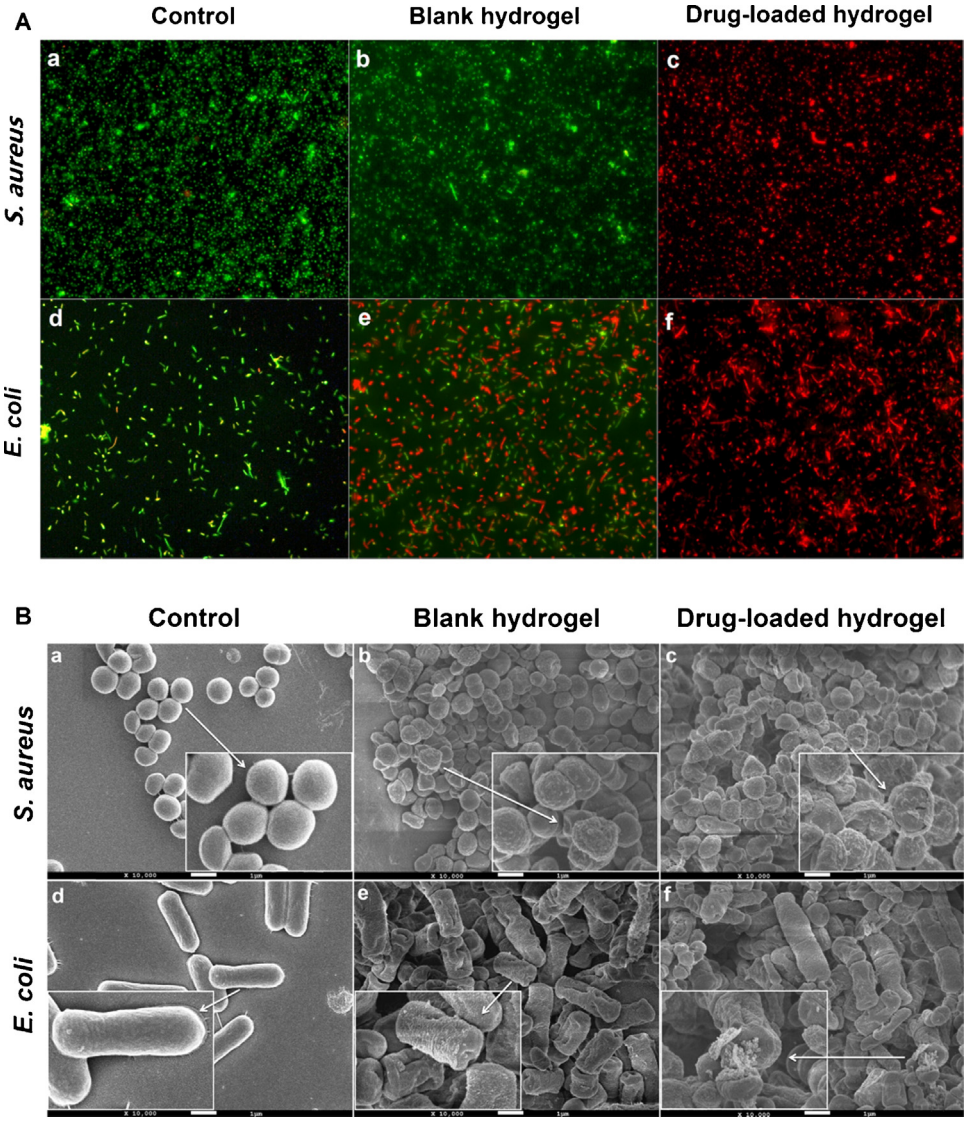

Fig. 5. Fluorescence micrograph of *E. coli* and *S. aureus* after being treated with CNDM hydrogels for 1 h (A); SEM images of *E. coli* and *S. aureus* after the treatment and no treatment of CNDM hydrogels, and arrow pointing micrographs indicate partially enlarged bacteria to observe surface information (B).

of the nutrients. That is, chitosan with high amino groups could not pass through the microbial membrane and hence stack to the cell surface, which blocked nutrient transport or permeated the microbial cell membrane, resulting in cell lysis.

For Gram-positive bacteria, the cell membrane was covered by a cell wall made up of 30–40 layers of peptidoglycans, which contained GlcNAc and *N*-acetylmuramic acid, to which the positively charged amino groups of chitosan can bind, resulting in cell wall disruption, and exudation of the cytoplasmic contents. In this situation, CS-NAc could not traverse the microbial membrane because of its large size and insolubility in water.

It is true that chitosan has high concentration of positive charge, and the deposition of cationic chitosan onto the cell surface, which leads to cell leakage, is more prominent in the case of Gram-negative bacteria, owing to a stronger association of O-chains to the outer membrane structure (Sajomsang, Tantayanon, et al., 2009).

To observe the bacterial morphology before and after treated with drug-loaded hydrogels, SEM was performed (Fig. 5B). For the bacteria without the treatment of the hydrogels, the cell surface presented smooth. In contrast, the bacteria after treated with hydrogels were shriveled, intracellular substances were even spilled from bacteria when dead (Fig. 5Bc and 5Bf).

4. Conclusions

A new biomimic hydrogel was formed using thiolated chitosan crosslinked with maleic acid-grafted dextran by Michael addition reaction. The hydrogels with porous structure had good swelling property. According to the contribution to cell proliferation, the hydrogels might promote wound healing. Hydrogels had antibacterial activity to Gram-negative bacteria and also had wide antibacterial properties after loading vancomycin. Moreover, vancomycin release presented a sustained pattern and was controlled via modifying the hydrogels compositions. Therefore, the polysaccharide hydrogels have promising and useful applications in biomedical devices.

Acknowledgments

This work was supported by the National Natural Science Foundation of China (Grant Nos. 21174071 and 81170773).

Appendix A. Supplementary data

Supplementary data associated with this article can be found, in the online version, at http://dx.doi.org/10.1016/j.carbpol.2014.01.068.

References

Agnihotri, S. A., & Aminabhavi, T. M. (2007). Chitosan nanoparticles for prolonged delivery of timolol maleate. *Drug Development and Industrial Pharmacy*, *33*, 1254–1262.

Brunel, F., Veron, L., David, L., Domard, A., Verrier, B., & Delair, T. (2010). Self-assemblies on chitosan nanohydrogels. *Macromolecular. Bioscience*, *10*, 424–432.

Brunel, F., Veron, L., Ladaviere, C., David, L., Domard, A., & Delair, T. (2009). Synthesis and structural characterization of chitosan nanogels. *Langmuir*, *25*, 8935–8943.

Bhattarai, N., Gunn, J., & Zhang, M. (2010). Chitosan-based hydrogels for controlled, localized drug delivery. *Advanced Drug Delivery Reviews*, *62*, 83–99.

Chen, C., Pan, F., Zhang, S., Hu, J., Cao, M., Wang, J., et al. (2010). Antibacterial activities of short designer peptides: A link between propensity for nanostructuring and capacity for membrane destabilization. *Biomacromolecules*, *11*, 402–411.

Dutta, S., Shome, A., Kar, T., & Das, P. K. (2011). Counterion-induced modulation in the antimicrobial activity and biocompatibility of amphiphilic hydrogelators: Influence of in-situ-synthesized Ag-nanoparticle on the bactericidal property. *Langmuir*, *27*, 5000–5008.

Haque, M. A., Kurokawa, T., & Gong, J. P. (2012). Super tough double network hydrogels and their application as biomaterials. *Polymer*, *53*, 1805–1822.

Jeong, B., Bae, Y. H., & Kim, S. W. (1999). Thermoreversible gelation of PEG–PLGA–PEG triblock copolymer aqueous solutions. *Macromolecules*, *32*, 7064–7069.

Jayakumar, R., Prabaharan, M., Kumar, P. T. S., Nair, S. V., & Tamura, H. (2011). Biomaterials based on chitin and chitosan in wound dressing applications. *Biotechnology Advances*, *29*, 322–337.

Kim, S. H., Won, C. Y., & Chu, C. C. (1999). Synthesis and characterization of dextran-maleic acid based hydrogel. *Journal of Biomedical Materials Research*, *46*, 160–170.

Krauland, A. H., Leitner, V. M., & Urch, A. B. S. (2003). Improvement in the in situ gelling properties of deacetylated gellan gum by the immobilization of thiol groups. *Journal of Pharmaceutical Sciences*, *92*, 1234–1241.

Kumar, P. T. S., Lakshmanan, V. K., Anilkumar, T. V., Ramya, C., Reshmi, P., Unnikrishnan, A. G., et al. (2012). Flexible and microporous chitosan hydrogel/nano ZnO composite bandages for wound dressing: In vitro and in vivo evaluation. *ACS Applied Materials & Interfaces*, *4*, 2618–2629.

Li, P., Poon, Y. F., Li, W., Zhu, H. Y., Yeap, S. H., Cao, Y., et al. (2011). A polycationic antimicrobial and biocompatible hydrogel with microbe membrane suctioning ability. *Nature Materials*, *10*, 149–156.

Mundargi, R. C., Patil, S. A., & Aminabhavi, T. M. (2007). Evaluation of acrylamide-grafted-xanthan gum copolymer matrix tablets for oral controlled delivery of antihypertensive drugs. *Carbohydrate Polymers*, *69*, 130–141.

Mundargi, R. C., Shelke, N. B., Rokhade, A. P., Patil, S. A., & Aminabhavi, T. M. (2008). Formulation and in-vitro evaluation of novel starch-based tableted microspheres for controlled release of ampicillin. *Carbohydrate Polymers*, *71*, 42–53.

Mitra, R. N., Shome, A., Paul, P., & Das, P. K. (2009). Antimicrobial activity, biocompatibility and hydrogelation ability of dipeptide-based amphiphiles. *Organic & Biomolecular Chemistry*, *7*, 94–102.

Madhumathi, K., Kumar, P. T. S., Abhilash, S., Sreeja, V., Tamura, H., Manzoor, K., et al. (2010). Development of novel chitin/nanosilver composite scaffolds for wound dressing applications. *Journal of Materials Science: Materials in Medicine*, *21*, 807–813.

Mao, S., Sun, W., & Kissel, T. (2010). Chitosan-based formulations for delivery of DNA and siRNA. *Advanced Drug Delivery Reviews*, *62*, 12–27.

Neto, C. G. T., Giacometti, J. A., Job, A. E., Ferreira, F. C., Fonseca, J. L. C., & Pereira, M. R. (2005). Thermal analysis of chitosan based networks. *Carbohydrate Polymers*, *62*, 97–103.

Paul, W., & Sharma, C. P. (2004). Chitosan and alginate wound dressings: A short review. *Trends in Biomaterials and Artificial Organs*, *18*, 18–23.

Rokhade, A. P., Patil, S. A., & Aminabhavi, T. M. (2007). Synthesis and characterization of semi-interpenetrating polymer network microspheres of acrylamide grafted dextran and chitosan for controlled release of acyclovir. *Carbohydrate Polymers*, *67*, 605–613.

Rokhade, A. P., Shelke, N. B., Patil, S. A., & Aminabhavi, T. M. (2007). Novel interpenetrating polymer network microspheres of chitosan and methylcellulose for controlled release of theophylline. *Carbohydrate Polymers*, *69*, 678–687.

Roy, S., & Das, P. K. (2008). Antibacterial hydrogels of amino acid-based cationic amphiphiles. *Biotechnology and Bioengineering*, *100*, 756–764.

Ryu, J. H., Lee, Y., Kong, W. H., Kim, T. G., Park, T. G., & Lee, H. (2011). Catechol-functionalized chitosan/pluronic hydrogels for tissue adhesives and hemostatic materials. *Biomacromolecules*, *12*, 2653–2659.

Sajomsang, W., Gonil, P., & Tantayanon, S. (2009). Antibacterial activity of quaternary ammonium chitosan containing mono or disaccharide moieties: Preparation and characterization. *International Journal of Biological Macromolecules*, *44*, 419–427.

Sajomsang, W., Tantayanon, S., Tangpasuthadol, V., & Daly, W. H. (2009). Quaternization of N-aryl chitosan derivatives: Synthesis, characterization, and antibacterial activity. *Carbohydrate Research*, *344*, 2502–2511.

Schutz, C. A., Lucienne, J. J., Kauper, P., & Wandrey, C. (2011). Cell response to the exposure to chitosan–TPP/alginate nanogels. *Biomacromolecules*, *12*, 4153–4161.

Song, A., Rane, A. A., & Christman, K. L. (2012). Antibacterial and cell-adhesive polypeptide and poly(ethylene glycol) hydrogel as a potential scaffold for wound healing. *Acta Biomaterialia*, *8*, 41–50.

Teng, D., Wu, Z., Zhang, X., Wang, Y., Zheng, C., Wang, Z., et al. (2010). Synthesis and characterization of in situ cross-linked hydrogel based on self-assembly of thiol-modified chitosan with PEG diacrylate using Michael type addition. *Polymer*, *51*, 639–646.

Tsao, C. T., Chang, C. H., Lin, Y. Y., Wud, M. F., Wanga, J. L., Han, J. L., et al. (2010). Antibacterial activity and biocompatibility of a chitosa-γ-poly (glutamic acid) polyelectrolyte complex hydrogel. *Carbohydrate Research*, *345*, 1774–1780.

Wang, X., Zheng, C., Wu, Z., Teng, D., Zhang, X., Wang, Z., et al. (2009). Chitosan-NAc nanoparticles as a vehicle for nasal absorption enhancement of insulin. *Journal of Biomedical Materials Research Part B: Applied Biomaterials*, *88B*, 150–161.

Wu, W., Shen, J., Banerjee, P., & Zhou, S. (2010). Chitosan-based responsive hybrid nanogels for integration of optical pH-sensing, tumor cell imaging and controlled drug delivery. *Biomaterials*, *31*, 8371–8381.

Zalfen, A. M., Nizet, D., Jerome, C., Jerome, R., Frankenne, F., Foidart, J. M., et al. (2008). Controlled release of drugs from multi-component biomaterials. *Acta Biomaterialia*, *4*, 1788–1796.

Zhang, H., Qadeer, A., & Chen, W. (2011). In situ gelable interpenetrating double network hydrogel formulated from binary components: Thiolated chitosan and oxidized dextran. *Biomacromolecules*, *12*, 1428–1437.

Zhang, L. F., Yang, D. J., Chen, H. C., Sun, R., Xu, L., Xiong, Z. C., et al. (2008). An ionically crosslinked hydrogel containing vancomycin coating on a porous scaffold for drug delivery and cell culture. *International Journal of Pharmaceutics*, *353*, 74–87.